Sensors and Materials, Vol. 37, No. 2 (2025) 783–794
MYU Tokyo

S & M 3956

Change Detection of Historical Villages in the Korean Demilitarized Zone Using a CNN Model: Focusing on Villages within the Korean Demilitarized Zone during the 1910s and 1950s

Haeyong Jeong*

Department of Geography Education, Kangwon National University
407, Education B/D 2, 1 Kangwondaehak-gil, Chuncheon-si, Gangwon-state 24341, Republic of Korea

(Received December 19, 2024; accepted February 21, 2025)

Keywords: demilitarized zone, deep learning, convolutional neural network, temporal-spatial analysis, historical topographic maps

In this study, we investigated the spatial and temporal changes in village distributions within the Korean Peninsula's Demilitarized Zone (DMZ) using deep learning methods. Historical maps from the 1910s and 1950s were analyzed to analyze house distributions and identify changes caused by historical events. A custom convolutional neural network model was developed for automated feature extraction, achieving high accuracy compared with traditional methods. The findings provide foundational data for understanding the historical continuity of settlements within the DMZ and aim to support future research on its restoration and development.

1. Introduction

With the signing of the "Korean Military Armistice Agreement (hereinafter referred to as the Armistice Agreement)" on July 27, 1953, the division of the Korean Peninsula was effectively established, and as a result, new boundaries and regions that had never existed before were formed. In the full text of Volume 1 and the maps in Volume 2 of the Armistice Agreement, boundaries and border areas such as the Military Demarcation Line, Demilitarized Zone (DMZ), and Han River Estuary Neutral Area are described and diagrammed in detail. The DMZ, formed around the Military Demarcation Line, has become a space where people can no longer reside.

The DMZ, which had been recognized as a residential area before the signing of the Armistice Agreement, began to be reexamined only after the year 2000, and studies concerning the region started to emerge. However, the investigation of villages that disappeared within the DMZ was conducted by superimposing a 1:50000 scale topographic map produced by the Japanese Government General of Korea in the 1910s to analyze the distribution of houses and villages in the 1910s. In this investigation, the number of houses and village size and

*Corresponding author: e-mail: wjdgofyd@kangwon.ac.kr
https://doi.org/10.18494/SAM5509

ISSN 0914-4935

characteristics were examined.[1–3] In this study, spatial data regarding houses were extracted and analyzed using the screen digitizing method, and village areas and sizes were derived through Thiessen polygon creation. However, screen digitizing consumes a significant amount of time because the scanned maps are georeferenced and researchers manually extract the coordinates of individual houses one by one.

On the other hand, the 1:50000 scale topographic map of the Korean Peninsula was measured three times. The third topographic map, referred to as the "Oman Basin Topographic Map," is the first official 1:50000 scale map produced using triangulation and consists of 722 map sheets. This map provides critical information about the Korean Peninsula in the early 1900s. Later, in the 1950s, the Volume 2 map of the Armistice Agreement, which revised the map produced during the Japanese colonial period, also provides important contemporary information.

Past maps contain historically, geographically, and economically significant information of an era.[4] These maps display Earth's surface as it existed in the past, with rich geographical features and high geographical accuracy, providing detailed information on elements such as ecology, urban structures, and natural landscapes. Such maps are valuable for conducting large-scale time-series analyses across various scientific disciplines, including urban planning, transportation, natural disasters, and archaeology.[5–9] The most critical task in utilizing such data is the accurate extraction of geographical features in digital data formats.[10] Typically, this involves digitizing scanned paper maps, a process that is time-consuming and costly.

To address these challenges, researchers have recently been adopting automated feature extraction methods, with deep convolutional neural network (CNN)-based models being proven highly efficient.[11] For example, Can *et al.*[4] conducted a study to automatically recognize various road types and their pixel-level locations using a CNN architecture on the third military map of the Austria–Hungary historical map series. Similarly, Xia *et al.*[11] investigated and compared three CNN-based texture map models with different feature extractors on the old national map of Switzerland: a pretrained VGG19 CNN, an autoencoder, and a hybrid model combining both. Additionally, Uhl *et al.*[10] conducted research on the extraction of human settlement patterns by applying CNN techniques to historical topographic maps of the U.S. Geological Survey. In Korea, however, no studies have applied CNN to the analysis of historical topographic maps. Previous studies primarily utilized the screen digitizing method, which did not fully account for time and spatial constraints.[1–3] The application of CNN to symbol extraction analysis on historical maps is expected to effectively overcome limitations related to time and spatial constraints.

The purpose of this study is to conduct a foundational investigation into houses distributed within the DMZ in the past. By identifying their spatial distribution and examining changes over time, we aim to provide a dataset of historical villages that can be used for future research. This work carries future-oriented value, serving as a basis for restoring the DMZ into a habitable area in the years to come.

2. Methods

2.1 Study area

The Military Demarcation Line was determined by the Armistice Agreement on July 27, 1953, and the areas retreating 2 km to the north and south from the Military Demarcation Line were designated as the DMZ. The DMZ has become a space where people can no longer settle down and live, and the records of this space are not easily obtainable. The ultimate goal of this research is to reinterpret these spaces and explain to current generations that they were spaces where many people lived even before the war, so that they can recognize them as spaces with historical continuity.

The area of the DMZ is 889.7 km^2, and its administrative districts include Paju-si and Yeoncheon-gun in Gyeonggi-do, and Cheorwon-gun, Yanggu-gun, Inje-gun, and Goseong-gun in Gangwon-do in South Korea and Kaesong-si, Cheorwon-gun, Pyeonggang-gun, Gimhwa-gun, Geumgang-gun, and Goseong-gun in Gangwon-do in North Korea. The 1:50000 scale topographic map consists of 20 map sheets from the 1910s and 9 map sheets from the 1950s, as shown in Fig. 1.

2.2 Overall methods

To achieve our research purpose, deep learning, an artificial neural network learning technique, was employed in machine learning and cognitive science, which is a statistical learning algorithm based on neural networks in biology.[12,13] Among these methods, we planned to use the CNN algorithm, a type of deep neural network, to create a distribution map of houses in the DMZ and its adjacent areas, and to detect changes by using period-based overlap analysis, as shown in Fig. 2.

To analyze disappeared villages within the DMZ, we collected maps from the 1910s and 1950s and performed georeferencing using the Arcgis 10.8 program to assign coordinates to the maps and conduct sampling. After completing the sampling, houses in the maps were extracted using a CNN model created through the eCognition program, and house distribution data were

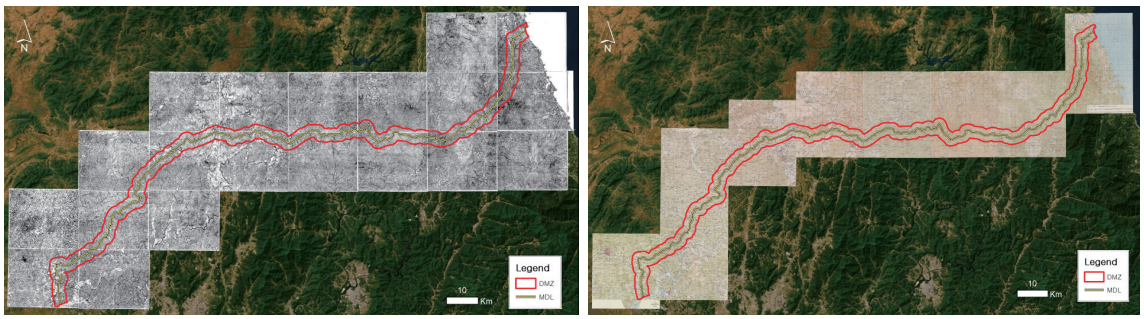

Fig. 1. (Color online) Extent of study area and location of selected map sheets for analysis.

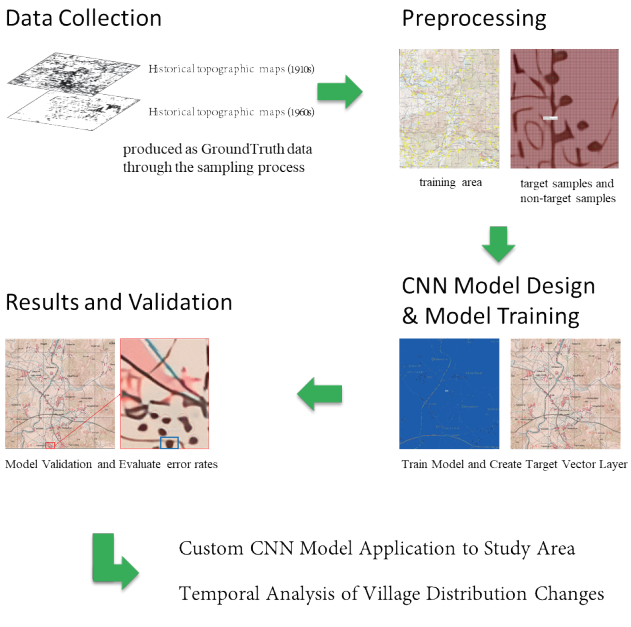

Fig. 2. (Color online) Overall methods.

constructed. Accuracy was improved through machine learning, and after confirming the results, the positional accuracy of the house distribution was maximized manually. Subsequently, Arcgis 10.8, a spatial analysis program, was utilized with the extracted data to derive results through overlap and change detection based on the distribution.

2.3 Step 1: Data collection and preprocessing

To analyze the disappeared villages in the DMZ, as a preparatory step, we first collected the 1:50000 topographic map of the Korean Peninsula produced in the 1910s and Volume 2 of the Armistice Agreement map produced in the 1950s. Then, using the ArcGIS 10.8 program, the military demarcation line was extracted from the 1950s map, the outskirts of the DMZ were extracted through buffer analysis, and the DMZ boundary was transformed into a polygon through modification. Afterwards, the maps of each era were georeferenced and coordinates were assigned to each map. The 1950s map was obtained from the U.S. National Archives, but owing to its low resolution, preprocessing graphics work was performed to physically increase the resolution. Data with high spatial resolution are very important for improving the analysis accuracy of CNN models.[14]

To detect disappeared villages, a sampling step was performed to identify and extract houses from historical topographic maps, which were produced as GroundTruth data through the sampling process. By defining the training area through the selection of a test area and overlapping the GroundTruth data, we used this training region for the validation of the CNN model.

In the training area, target and nontarget samples were classified, as shown in Fig. 3. Target samples correspond to houses, and nontarget samples correspond to other symbols. In this manner, each dot symbol representing a house was divided into individual objects, labeled, and prepared as data for CNN-based feature extraction. This preprocessing step is essential to ensure that the model can accurately identify house locations and distinguish them from other map symbols.

2.4 Step 2: Model architecture design (custom CNN model for geospatial analysis)

The eCognition program's CNN analysis architecture is designed primarily for object-based image analysis, focusing on detecting specific symbols on topographic maps and extracting their features. Therefore, it provides an extremely effective model structure for this study. Compared with other architectures such as LeNet, AlexNet, VGGNet, GoogleNet, ResNet, DenseNet, and DPN—primarily designed for general image classification and object recognition tasks—this architecture is more suitable for geospatial data analysis. It is optimized for detecting symbolic features on topographic maps and adopts a single-layer architecture, enabling faster and more efficient detection of target patterns and symbols. This approach also captures the spatial information surrounding each point.

The CNN model architecture used in this study consists of an input layer, a convolutional layer with a relatively large kernel, a max pooling layer, and an output layer that generates a probability heatmap for the presence of the target object (house).[15–17] Each layer performs a specific function in the detection process, allowing the model to capture the spatial patterns necessary for accurately identifying the distribution of village houses.

The input layer receives preprocessed 14 × 14 pixel patches, enabling the model to recognize fine-grained patterns within map segments. This 14 × 14 pixel size serves as the basis for the typical spatial resolution analysis of houses on a 1:50000 scale map.

The convolutional layer applies a 7 × 7 kernel, producing 40 feature maps. By performing this convolution operation 40 times using different kernels, we can generate unique feature

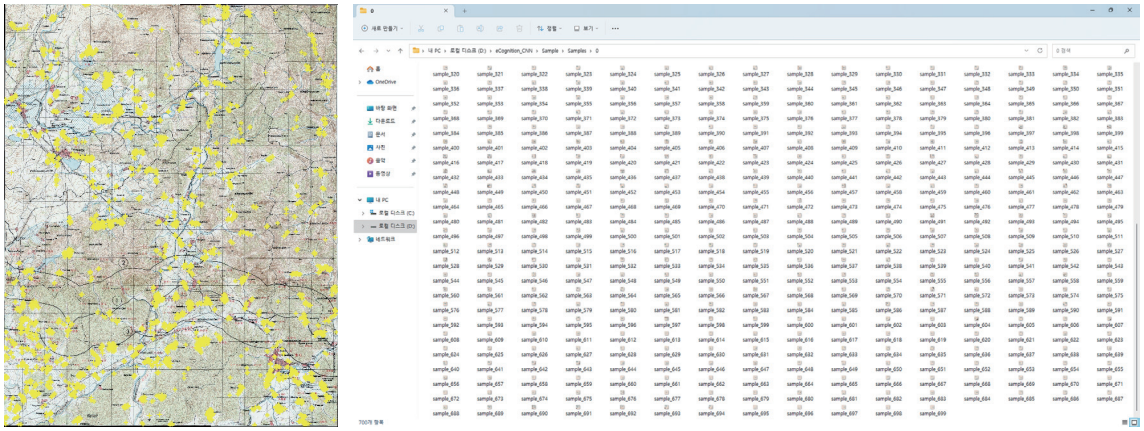

Fig. 3. (Color online) Sample load (thematic map) and creation of samples.

maps, capturing patterns such as house shape, density, and alignment. Through this, the model can learn to distinguish houses from other symbols. The convolutional layer operation follows Eq. (1).

$$Y = [i, j] = \sum_{m=1}^{7}\sum_{n=1}^{7} X[i+m, j+n] \cdot W[m,n] + b \tag{1}$$

$Y[i, j]$ is the output feature map at position (i, j), $X[i + m, j + n]$ represents the input values from the 7 × 7 neighborhood around position (i, j) in the input patch, $W[m, n]$ is the weight of the convolutional kernel at position (m, n), and b is the bias term added to each convolutional operation.

Following the convolutional layer, a max pooling layer is applied to reduce the spatial dimension of the feature maps. This step excludes irrelevant information, retains only the most salient features, and enhances the model's robustness. It is the most important step in spatial analysis, playing a crucial role in preserving the extracted house locations by removing parts that do not contribute to house detection. With the reduced computational burden, it allows the model to process large amounts of map data more efficiently. The max pooling operation, generally applied with a 2 × 2 pooling window, selects the maximum value within each subregion of the map, with related operations following Eq. (2).

$$Y'[i, j] = \max(X[i : i+2, j : j+2]) \tag{2}$$

$Y'[i, j]$ is the pooled output and $X[i : i + 2, j : j + 2]$ represents a 2 × 2 region in the feature map from the convolutional layer.

The final layer is the output layer, which generates a location-based probability heatmap representing the likelihood of a house being present across the patch. This provides a visual representation of the spatial distribution of detected houses, with higher values indicating a higher probability of target presence. This approach makes the distribution of villages over time directly interpretable, facilitating geospatial analysis and change detection. The output heatmap is generated using a softmax or sigmoid activation function, depending on whether multiclass or binary detection is required. In this case, it appears that the sigmoid function is used to calculate the probability of target presence.

2.5 Step 3: Training of model (custom CNN model)

Training consists of numerous individual training steps. In each step, a randomly selected batch of samples is input into the model, gradients for each weight are calculated using backpropagation, and the weights are optimized using statistical gradient descent. In this training, the learning rate was set to 0.0006, the number of training steps was set to 5000, and the batch size, which is the number of samples used in each training step, was set to 50. The learning rate is a very important parameter. If it is too low, not only does the training process become slow, but there is also a risk of getting stuck in local minima without reaching near-

optimal weights. If it is too high, the model may initially improve quickly, but it may not be able to reach the bottom of the minimum and may simply "jump" around it. When the model is applied through CNN training, the model is created as a heatmap layer, as shown in Fig. 4. On the basis of this layer, pixels (houses) classified as targets are analyzed.

2.6 Step 4: Model validation and evaluation of error rates

Through model training, the locations of houses were compared against the original GroundTruth data. In the training area (3000 × 5000 pixels), where there are a total of 183 houses in the GroundTruth data, 182 houses were displayed through model training, yielding a Miss value of 1, as shown in Fig. 5 and an overall error rate of 99.45%. This value was calculated by setting the threshold to 0.9. When the value was less than 0.9, more points appeared on the line based on vector data, and when it exceeded 0.9, fewer house points appeared. Regarding the error rate, the following equation was used.

$$Error\ Rate = \frac{Error}{Total\ Number\ of\ Samples} \gg Error\ Rate = \frac{False + Miss}{Hit + False + Miss} \tag{3}$$

2.7 Step 5: Custom CNN model application to study area

The model, which was applied on the basis of the training area, was then sequentially applied to the nine map sheets that comprise the study area. The results were tested again on the Pyeonggang map sheet, from which the GroundTruth data were extracted but were not part of the training area. Out of 3288 houses, 3188 houses (Hit value) matched, and 100 houses were Miss values. A False value meant that there was no overlap. The accuracy was approximately 97%. This model was applied to each of the remaining eight map sheets and the houses extracted from each map sheet were converted into vector files, as shown in Fig. 6.

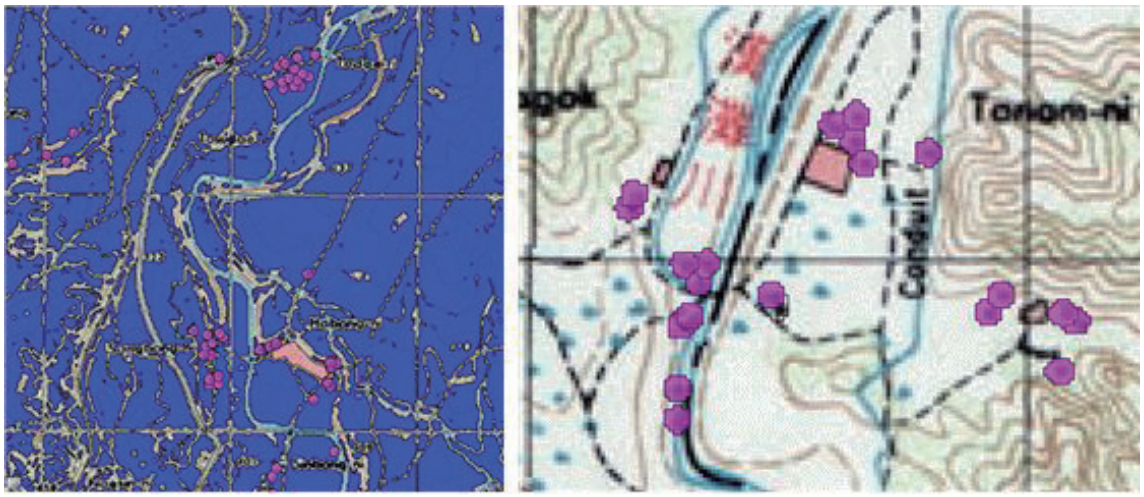

Fig. 4. (Color online) Model training and creation of target vector layer.

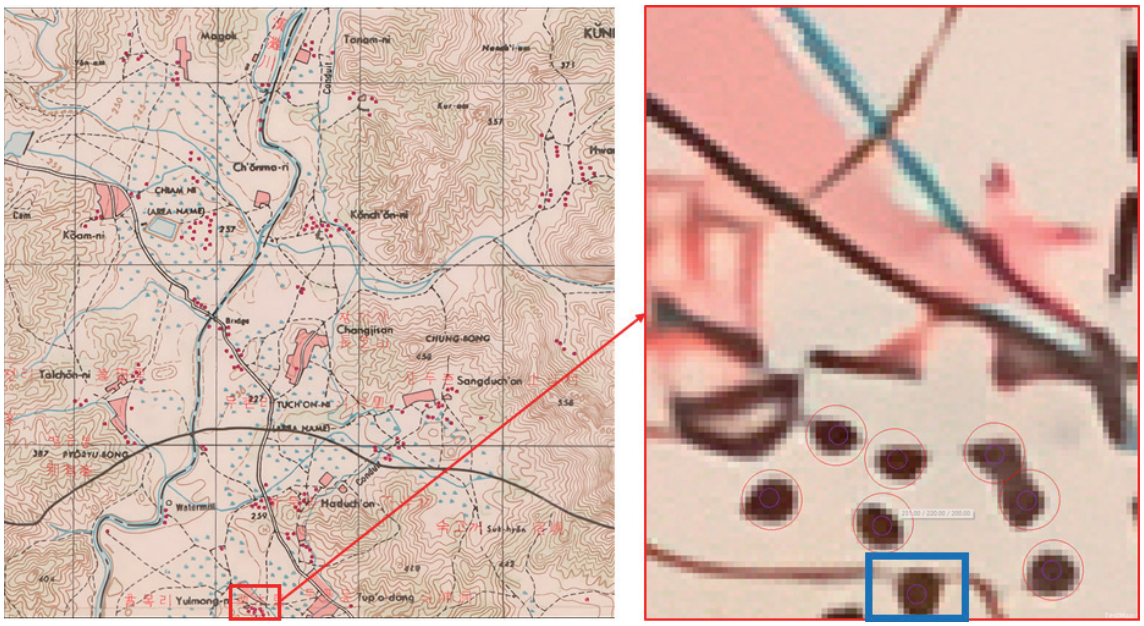

Fig. 5. (Color online) Miss value in the training area.

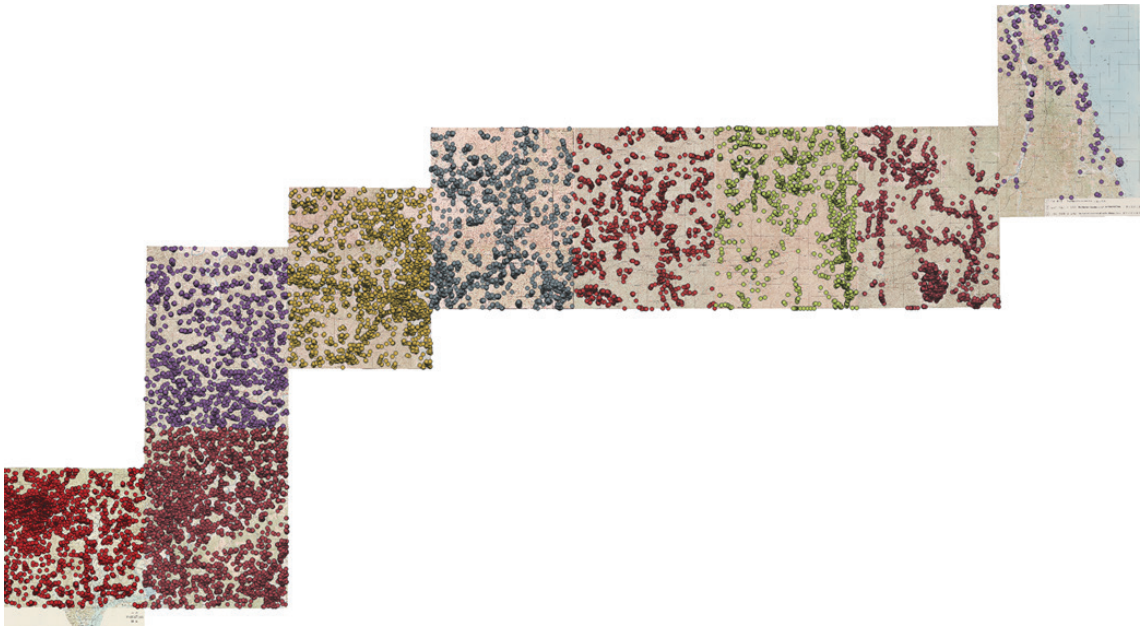

Fig. 6. (Color online) Results of applying nine map sheets to CNN model.

3. Results: Temporal Analysis of Village Distribution Changes

Using the Arcgis 10.8 program, we extracted only the house data inside the DMZ from the house data of the nine map sheets obtained by applying the Custom CNN model, and a single

DMZ house dataset was created using the Merge tool. This dataset represents the houses in the DMZ in the 1950s. The house data for the 1910 topographic map were created by vectorizing and then excluding the urban area of the 1950s. These two datasets were then analyzed for changes using kernel density analysis and overlap analysis, and the distribution pattern of houses was confirmed by comparing their density distribution within the DMZ. The change in the number of houses by administrative district in the DMZ is presented in Table 1. In Gyeonggi-do, the number of houses appears to have decreased owing to the incorporation of houses into city areas, resulting from urban expansion.

In Gangwon-do, the number of houses increased, particularly around Cheorwon; in contrast, Goseong experienced a reduction of more than half. This difference is likely due to the concentration of houses around the plains. In the case of Goseong, it is suggested that the reduction in the number of houses is related to their incorporation into the expanding city boundaries.

Table 1
Results of changes in the regional distribution of houses (units) in the DMZ.

Category	Total	Gyeonggi	Paju	Yeoncheon	Gangwon	Cheor-won	Yanggu	Inje	Change
1910s	4188	1894	669	1225	2294	1550	265	176	303
1950s	4015	1682	476	1206	2333	1777	212	201	143
Change	−173	−212	−193	−19	+39	+227	−53	+25	−160

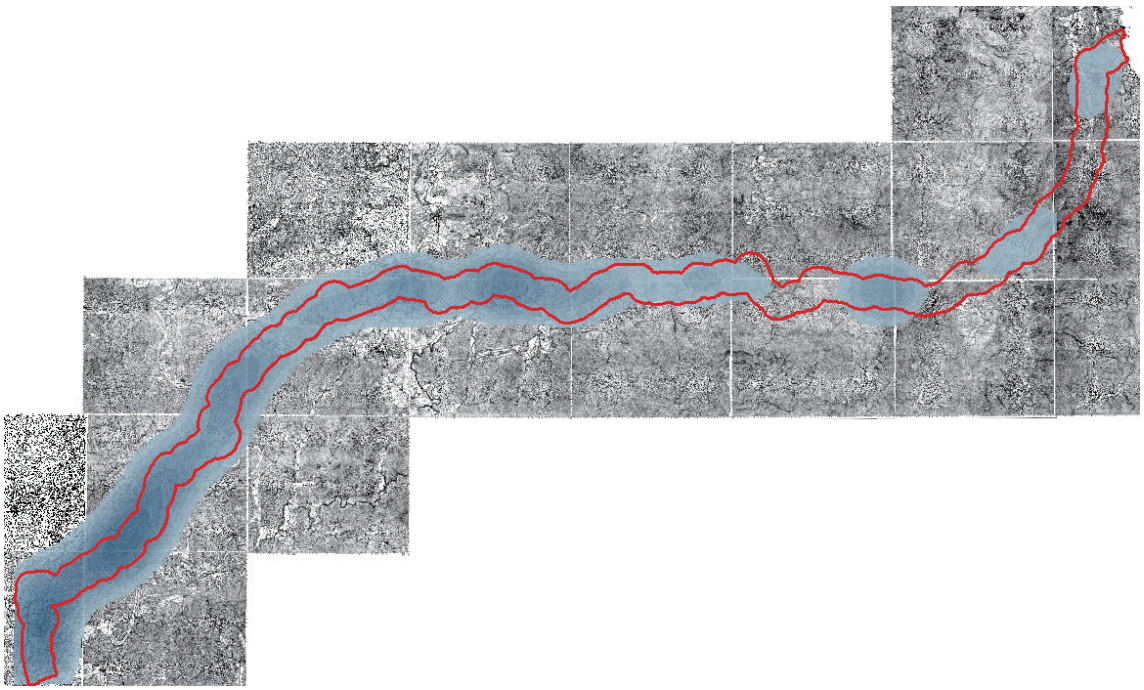

Fig. 7. (Color online) Results of house density analysis in the 1910s.

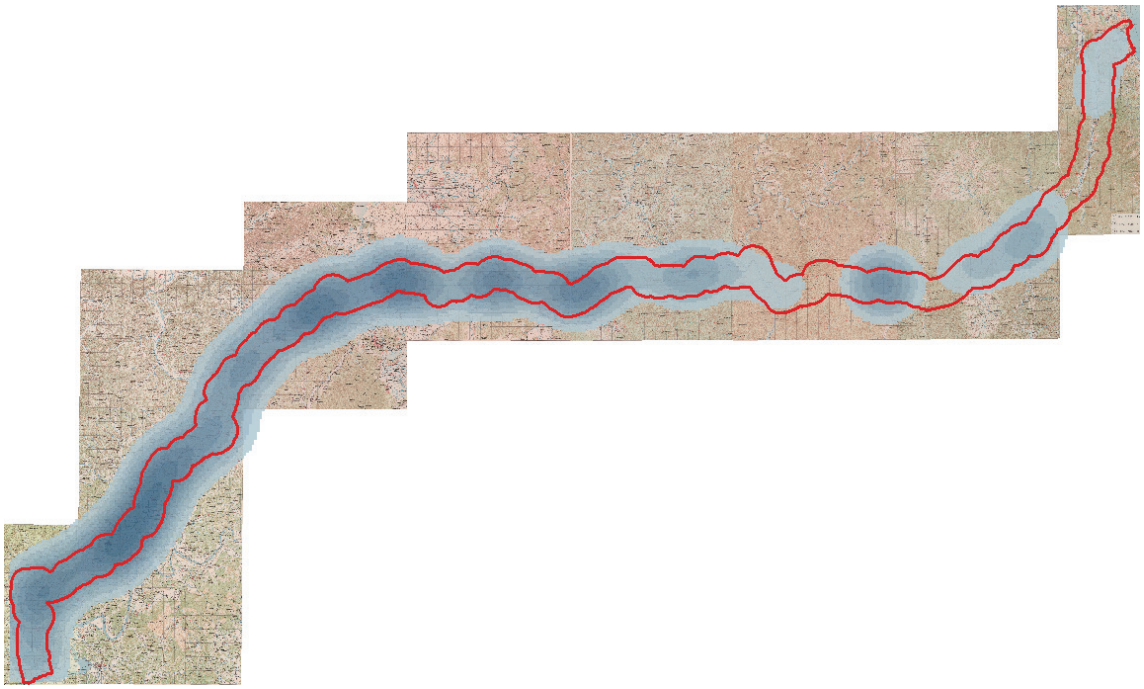

Fig. 8. (Color online) Results of house density analysis in the 1950s.

In the 1910s, according to the administrative districts of South Korea, houses were concentrated in nine areas: Sagok, Kaeseong-si, Gyeonggi-do; Hangdong-ri–Bangnae-dong and Yangjimal, Yeoncheon-gun; Woljeong-ri, Yugok-ri, and Soseong-dong, Gangwon-do; Mundeung-ri, Yanggu-gun; Jangseung-ri, Inje-gun; and Oemyeon-ri, Goseong-gun, as shown in Fig. 7. However, in the 1950s, houses were concentrated in eleven areas: Daeseong-dong, Paju-gun; Hangdong-ri–Bangnae-dong, Yeoncheon-gun; Yangjimal, Daemari, Cheorwon-gun; Woljeong-ri, Yugok-ri, Sinmok-dong, Soseong-dong, Mundeung-ri, Yanggu-gun; Jangseung-ri, Inje-gun; and Oemyeon-ri, Goseong-gun, confirming that the population distribution expanded more east–west than before, as shown in Fig. 8. What these regions have in common is that they have well-developed roads and rivers connecting north and south, making it easier to expand houses.

4. Discussion and Conclusions

In this study, we constructed house data by creating and applying a custom CNN model to villages that disappeared in the DMZ, and used these data to compare house and village patterns according to the distribution of houses in the DMZ. Data were constructed more easily and quickly through the creation of the CNN model than through manual methods of existing vectorization. In the error rate verification, an accuracy exceeding 97% was achieved, and it is expected that future data construction research using CNN models will be able to provide more accurate and easy-to-use basic data.

However, through this study, several points requiring improvement were identified for constructing point data within vector data. To build sample data, such as the initial GroundTruth data, it is necessary to have a topographic map with improved resolution, and when constructing GroundTruth data, the "Point" must be displayed precisely at the very center. Through this process, more accurate analysis and data acquisition will be possible. One must also clearly understand the settings for the second preprocessed pixel patch value and the threshold value, and input the corresponding values. This is because applying preprocessed pixel patch values and threshold values is crucial for ensuring accuracy and reducing analysis time. In this study, a preprocessed 14 × 14 pixel patch was applied, and the threshold value was set to 0.9, resulting in highly accurate data. The 14 × 14 pixel patch is best suited for point extraction on the map, and if it is larger, similar symbols are detected. The smaller than 0.9, the more unnecessary symbols were detected, and such symbols were not extracted. In the case of learning rates and training phases, model operation speed and analysis accuracy were set to the closest value. Adjustment of these values was determined to be the most suitable for house extraction on the map.

Lastly, there is the issue of data unification for time series analysis. To align the data, a unified analysis based on newly constructed data rather than previous data is required. In this study, existing data were modified and used because of the low resolution of the 1910s map. It is evident that there is an error in this regard. Furthermore, since accurate house data values for built-up areas formed owing to urban expansion did not exist, data on these built-up areas were excluded, limiting the analysis results for house and village patterns. In the future, it will be necessary to explore various methods to address these issues in order to reconstruct the past and contribute to research.

This is the first study exploring the discovery and use of data with deep learning from a geographical perspective. Given that research on disappeared villages and the extraction of related data are not actively pursued, and that there is insufficient research on how to efficiently extract such data, we focused on the geographical aspect of research on the distribution and change detection of disappeared villages through deep learning. It is anticipated that it will contribute to providing more accurate and user-friendly basic data through the sharing of research results based on the constructed database.

Acknowledgments

This study was supported by 2021 Research Grant from Kangwon National University.

References

1 C. H. Kim: J. Korean Assoc. Geogr. Inf. Stud. **12** (2009) 96.
2 C. H. Kim: J. Korean Assoc. Geogr. Inf. Stud. **22** (2019) 19. http://dx.doi.org/10.11108/kagis.2019.22.1.019
3 H. Y. Jeong: J. Korean Assoc. Geogr. Inf. Stud. **22** (2019) 114. http://dx.doi.org/10.11108/kagis.2019.22.1.114
4 Y. S. Can, P. J. Gerrits, and M. E. Kabadayi: IEEE Access **9** (2021) 62847. https://doi.org/10.1109/ACCESS.2021.3074897
5 M. Heitzler and L. Hurni: ICA-Abs **1** (2019) 1. https://doi.org/10.5194/ica-abs-1-110-2019
6 M. Saeedimoghaddam and T. F. Stepinski: Int. J. Geogr. Inf. Sci. **34** (2020) 947. https://doi.org/10.1080/13658816.2019.1696968

7 T. Martinez, A. Hammoumi, G. Ducret, M. Moreaud, R. Deschamps, H. Piegay, and J. F. Berger: J. Maps **19** (2023) 1. https://doi.org/10.1080/17445647.2023.2225071
8 B. Ekim, E. Sertel, and M. E. Kabadayı: ISPRS Int. J. Geo-Inf. **10** (2021) 1. https://doi.org/10.3390/ijgi10080492
9 C. Henry, S. M. Azimi, and N. Merkle: IEEE Geosci. Remote Sens. Lett. **15** (2018) 1867. https://doi.org/10.1109/LGRS.2018.2864342
10 J. H. Uhl, S. Leyk, Y. Y. Chiang, W. Duan, and C. A. Knoblock: IEEE Access **8** (2020) 6978. https://doi.org/10.1109/ACCESS.2019.2963213
11 X. Xia, M. Heitzler, and L. Hurni: ISPRS **13** (2020) 1167. https://doi.org/10.5194/isprs-archives-XLIII-B2-2022-1167-2022
12 W. S. Oh, W. G. Lee, and J. S. Oh: J. Korean Inst. Gas **22** (2018) 8. http://dx.doi.org/10.7842/kigas.2018.22.6.8
13 T. Kikuchi, K. Sakita, S. Nishiyama, and K. Takahashi: Nat. Hazard. **117** (2023) 339. https://doi.org/10.1007/s11069-023-05862-w
14 K. Simonyan and A. Zisserman: ICLR 2015 Conf. (ICLR, 2015) 1–15. https://doi.org/10.48550/arXiv.1409.1556
15 K. He, X. Zhang, S. Ren, and J. Sun: arXiv **4** (2015) 1. https://doi.org/10.48550/arXiv.1406.4729
16 C. Yu, R. Han, M. Song, C. Liu, and C.-I. Chang: IEEE Trans. Geosci. Remote Sens. **60** (2022). https://doi.org/10.1109/TGRS.2021.3058549
17 Z. Shao, X. Chen, L. Du, L. Chen, Y. Du, W. Zhuang, H. Wei, C. Xie, and Z. Wang: IEEE Trans. Circuits Syst. I Regul. Pap. **69** (2022) 668. https://doi.org/10.48550/arXiv.2110.06155

About the Authors

Hae Yong Jeong received his B.S. degree from Kangwon National University, Republic of Korea, in 2003 and his M.S. and Ph.D. degrees from Kangwon National University, Republic of Korea, in 2011 and 2017, respectively. Since 2019, he has been a professor at Kangwon National University, Republic of Korea. His research interests are in GIS, regional geography, and sensors. (wjdgofyd@kangwon.ac.kr)